Measurement of material nonlinearity using surface acoustic wave parametric interaction and laser ultrasonics

Theodosia Stratoudaki,[a] Robert Ellwood, Steve Sharples, Matthew Clark, and Michael G. Somekh
Division of Electrical Systems and Optics, Faculty of Engineering, University of Nottingham, Nottingham NG7 2RD, United Kingdom

Ian J. Collison
NDE General Office, Rolls-Royce plc, Elton Road, Derby DE24 8BJ, United Kingdom

(Received 13 August 2010; revised 30 January 2011; accepted 10 February 2011)

A dual frequency mixing technique has been developed for measuring velocity changes caused by material nonlinearity. The technique is based on the parametric interaction between two surface acoustic waves (SAWs): The low frequency pump SAW generated by a transducer and the high frequency probe SAW generated and detected using laser ultrasonics. The pump SAW stresses the material under the probe SAW. The stress (typically <5 MPa) is controlled by varying the timing between the pump and probe waves. The nonlinear interaction is measured as a phase modulation of the probe SAW and equated to a velocity change. The velocity–stress relationship is used as a measure of material nonlinearity. Experiments were conducted to observe the pump–probe interaction by changing the pump frequency and compare the nonlinear response of aluminum and fused silica. Experiments showed these two materials had opposite nonlinear responses, consistent with previously published data. The technique could be applied to life-time predictions of engineered components by measuring changes in nonlinear response caused by fatigue.
 [DOI: 10.1121/1.3560945]

PACS number(s): 43.25.Dc, 43.25.Fe, 43.40.Le [ROC] Pages: 1721–1728

I. INTRODUCTION

Nondestructive evaluation (NDE) is essential in many industrial sectors, especially for safety critical applications such as aerospace or nuclear industries. The motivation behind NDE is to provide reliable products by minimizing the risk of failure thereby reducing costs and maximizing safety. NDE is used to characterize materials, monitor manufacturing processes, and detect defects. Some of the most important but difficult to detect defects include contacting defects, defected diffusion bonds, or disbonded delaminations that are precursors of critical damage. Ultrasound is one of the most widely used and powerful NDE techniques. Traditional linear ultrasonic methods (e.g., reflection, diffraction from cracks, changes in attenuation or velocity) are capable of successfully detecting gross cracks, but they are insensitive to detecting microscale defects. Defects and precursors of damage such as microcracks and dislocations can be regarded as nuclei of the fracture process and since they are much smaller than the acoustic wavelength at the frequencies generally used for NDE, general degradation of a component can be very well hidden and degraded materials can pass for flawless under standard ultrasonic tests. On the other hand, microcracks and dislocations give rise to excess material nonlinearity providing earlier indications of failure than those given by linear ultrasonic techniques,[1,2] with the potential of making "life-time" predictions.[3,4]

There are numerous experimental techniques used for measuring material nonlinearity.[5] The higher harmonic generation method measures the harmonic content of a single ultrasonic wave.[6] The technique has been applied to various materials including composites[7–9] and to measure fatigue.[10,11] More recent methods include nonlinear time reversal[12–14] and nonlinear reverberation.[9]

The majority of published work in nonlinear ultrasonics is performed with bulk waves.[15] However, the use of ultrasound to detect the presence of defects is not limited to the interior of materials and defects located on or near the surface of materials are more effectively detected using surface acoustic waves (SAWs). SAWs have been used extensively for NDE purposes such as detecting surface-breaking fatigue cracks[16,17] and measuring stress.[18–21] Recently, the nonlinear harmonic generation technique has been performed with a SAW.[4,22–24]

Another family of nonlinear ultrasonic techniques is the measurement of parametric interaction.[25] In a nonlinear material, a propagating wave is affected (either frequency modulation[26,27] or phase modulation[28,29]) by the presence of a second wave or vibration. The nonlinear technique presented in this article is based on parametric interaction between a "pump" and a "probe" wave and the material nonlinearity manifests itself as a modulation of the probe signal. The technique has been demonstrated using longitudinal waves and recently using Lamb waves.[30] The acoustic waves have been generated using various means (e.g., modulating vibration[10,11] using contact transducers[28,29] or with an impact hammer or shaker[31–33]) and materials examined with this method include polystyrene, aluminum, titanium, and fused silica.[28,29]

[a]Author to whom correspondence should be addressed. Electronic mail: T.stratoudaki@nottingham.ac.uk

The experiments presented in this article are based on the parametric interaction between a transducer generated pump SAW and a laser generated probe SAW. We have previously demonstrated the potential of this technique using cheap optical transducers (CHOTs) for generation and detection of ultrasound[34] and we now show its capabilities to measure material nonlinearity using laser ultrasonics. Laser ultrasound can overcome several shortcomings associated with the use of contact transducers: It is a remote and couplant free technique especially suitable for components with complex geometry and places with restricted access.

In this article we present, the experimental instrumentation that has allowed accurate measurements of velocity changes due to the frequency mixing of the pump and probe waves (Sec. II), the method we used to analyze our data (Sec. III), and experimental results that confirm the capability of this technique to measure material nonlinearity (Sec. IV).

II. NONLINEAR EXPERIMENTAL CONFIGURATION

Experiments were performed using three different transducers (0.5, 1, and 2 MHz) to excite the pump SAW. The probe SAW was 78 MHz for the experiments on fused silica and 67 MHz for those on aluminum. It was generated using an amplitude mask/laser combination. The SAWs were detected optically by means of a knife-edge detector for the probe wave and a Polytec vibrometer for the pump wave. The pump SAW packet was typically 6, 3, and 1.5 μs in duration, approximately a three-cycle packet of a 0.5, 1, and 2 MHz signal, respectively, and the probe SAW packet was approximately 0.25 μs duration (measured at FWHM). Since the pump wave was longer than the probe signal, the degree of phase modulation experienced by the probe depended on which portion of the pump wave it interacted with. In order to see changes in the phase response of the probe signal, its point of interaction with the pump wave was altered. This was achieved through accurate time control electronics to delay the triggering time of the probe pulse with respect to the pump.

A. Instrumentation

The essential elements of the experimental apparatus are shown in Fig. 1 and can be broken down into four sections.

1. Low frequency pump generation (A in Fig. 1)

The transducer was attached to a wedge so as to excite the pump SAW onto the sample surface. The transducer, wedge, and sample were bonded together with phenyl salicylate glue. NDT-tech transducers with center frequencies of 0.5 MHz (A414S-SB), 1 MHz (A402S-SB), and 2.25 MHz (A404S-SB) were used. The transducer driving signal was generated by the Agilent 33250A arbitrary waveform generator. This device was externally triggered by the timing electronics, and on each

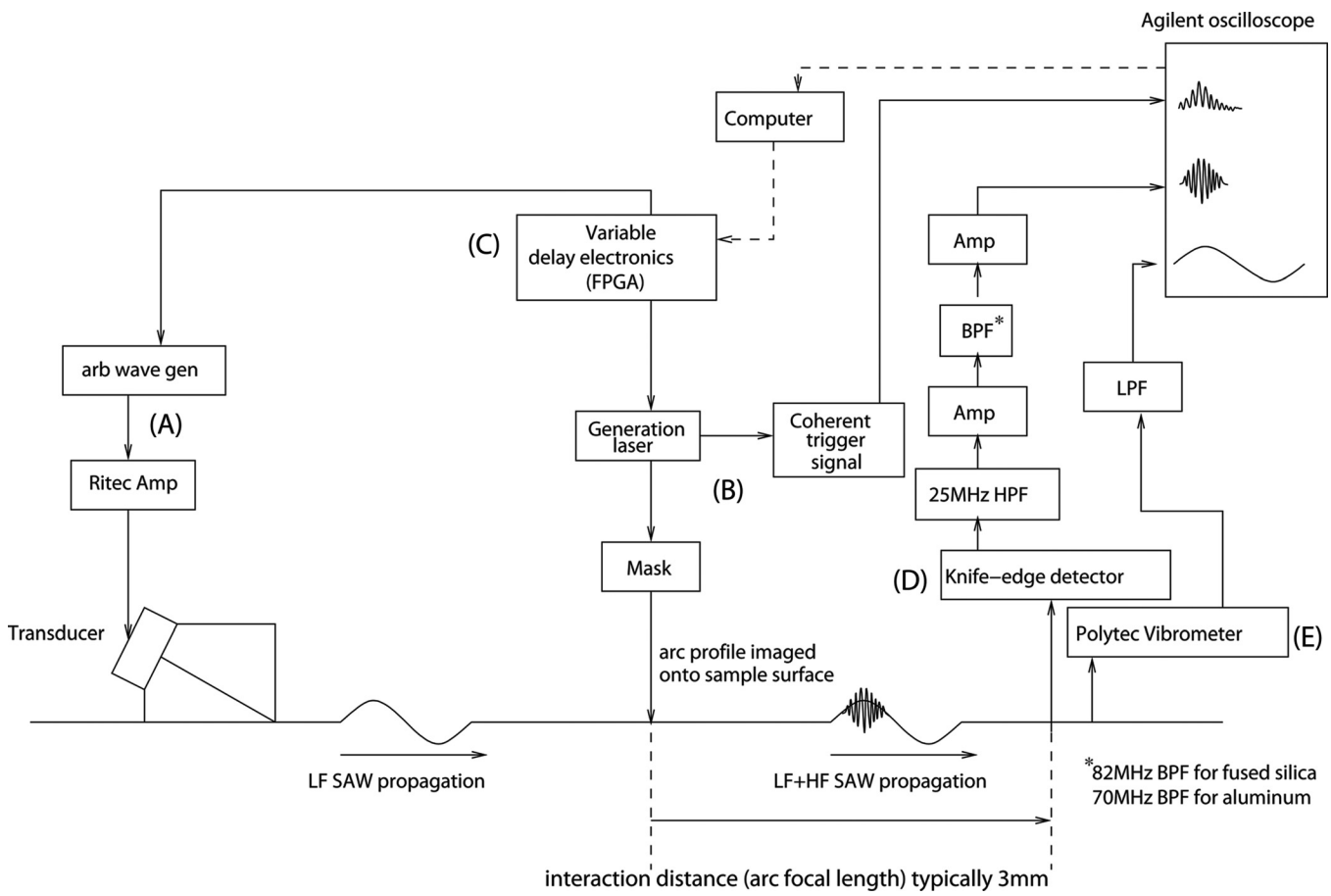

FIG. 1. Schematic of the nonlinear experiment configuration. Low frequency pump section (A), high frequency probe section (B), delay control electronics (C), detection section (D) and (E).

trigger event a three-cycle sine wave with a peak-to-peak amplitude in the range of 0.450 V was generated. This signal was amplified by a Ritec RPR-4000 gated amplifier giving burst with peak-to-peak amplitudes of 532 V. The frequency range over which the driving amplifier was most powerful was 0.5–2 MHz.

2. High frequency probe generation (B in Fig. 1)

The generation laser was a Q-switched infrared laser emitting light at a wavelength of 1064 nm. A photodetector placed at the output of the laser provided a coherent trigger pulse. The laser pulse had a rise time of 8 ns and frequency content that extended up to 80 MHz. The laser illuminated the amplitude mask which blocked part of the laser beam and manipulated the light distribution on the sample surface (Fig. 2). The pattern of the mask consisted of a series of arcs separated by 116 μm. The approximate size of the laser beam on the sample surface after focusing was 1 mm^2 and the arcs pattern, after imaging, had a separation of 43.5 μm, corresponding to the ultrasonic wavelength. The generated wave had thus a frequency of $f = v/\lambda$, where v is the Rayleigh wave velocity and λ is the acoustic wavelength or arc separation.

3. Delay control electronics (C in Fig. 1)

The timing of the experiment was controlled by a single master clock signal implemented on a field programmable gate array (FPGA). The delay resolution between events was 10 ns and the chosen delay increment was 80 ns corresponding to a 0.25, 0.5, and 1 rad of phase step for the 0.5, 1, and 2 MHz pump waves. The FPGA generated two output signals. The delay between these signals was computer controlled and set the time at which the pump and probe sources were generated. The two generated SAWs propagated over the sample, interacting with each other over a distance of 3 mm, after which they were detected. The phase modulation of the high frequency caused by interacting with the low frequency was then measured.

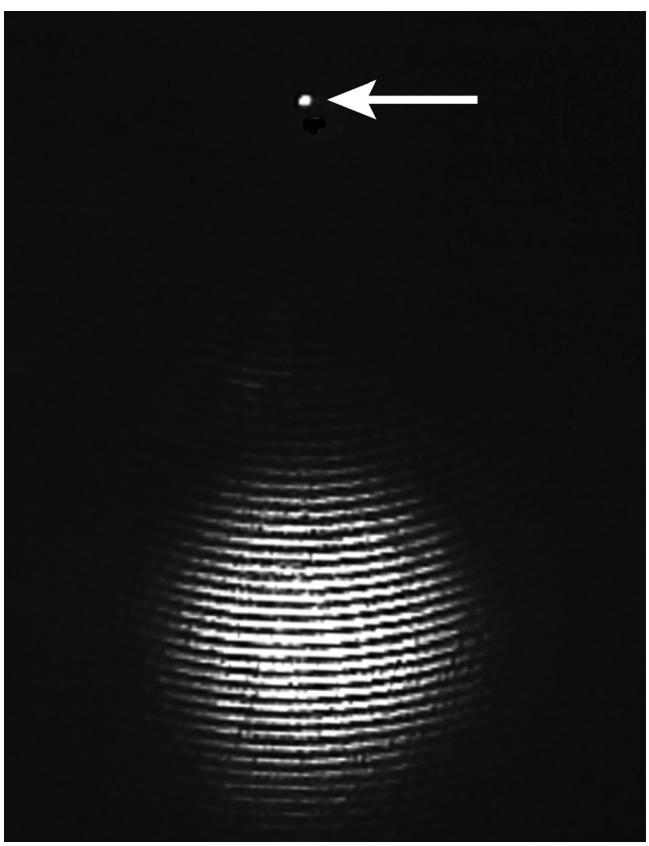

FIG. 2. Image of the generation beam on the sample surface. The bright spot at the top middle, indicated by the arrow, is the knife-edge laser detection beam.

4. Signal detection (D and E in Fig. 1)

We used a knife-edge detector[35] with broadband electronics (400 kHz–450 MHz) for the detection of the high frequency probe signal. The beam of a 644 nm CW diode laser was reflected from the sample surface and deflected between two photodiodes when the surface of the sample was displaced by a passing SAW. The low frequency pump SAW was measured very close to the detection site for the probe signal using a calibrated Polytec vibrometer (bandwidth 30 kHz–24 MHz). The small difference in position of the detection sites of the Polytec vibrometer and the knife edge and different delays in the electronics, introduced a small ($= 30°$) phase difference between the detected pump and probe signal. This was removed before further data analysis.

B. Suppression of temperature effects: Interlacing differential data acquisition

Changes in laboratory temperature, even by as little as $\pm 1°$ C, overwhelmed the nonlinear measurements. Temperature change affected the experiment in two ways:

(1) Ultrasound velocity is dependent on sample temperature.[36]
(2) The expansion and contraction of equipment caused changes in the geometrical setup of the apparatus.

Experiments lasted for approximately 40 min and although the laboratory ambient temperature was controlled by an air conditioning system, temperature variations introduced phase changes of at least 0.2 rads corresponding to the velocity changes of 1.5 ms^{-1}. This was a significant problem since it was found that the phase modulation caused by the nonlinearity of the materials we tested was at least ten times smaller. As a result, in order to observe this phase modulation, the effect of temperature had to be suppressed.

To minimize the effect of temperature, an interlacing differential data acquisition technique was developed. This technique measured the phase difference between a "reference" delay taken at a time when the pump and probe waves had not interacted and a "target" delay taken at a suitable pump and probe interaction time. Both sets of data were acquired simultaneously using a single oscilloscope by switching between them (interlacing). For this reason, two channels of the oscilloscope were used to capture the data: One for the reference measurement and one for the stressed measurement. The signal from the detector was rapidly switched (30 Hz) between the two channels under the control of the FPGA which synchronized this with the changing of the delay of the low frequency pump. This effectively

switched the stress on and off by moving the interaction time. Since the effect of temperature is relatively slow, the effect of stress on the velocity of the probe beam could be reliably assessed by the difference between the reference and stress measurements. Averaging this value allows the effects of random noise to be reduced.

Figure 3(a) shows the phase of the reference and target signals captured before being subtracted and demonstrates the effect of temperature on the data while Fig. 3(b) shows the same set of data when the phase of the target has been subtracted from that of the reference, the temperature effect has been suppressed and the phase modulation due to the stress caused by the pump wave is apparent.

III. DATA ANALYSIS

Our aim was to measure the velocity modulation ΔV_{HF} over stress. The raw data consisted of a number of detected probe SAW signals that had interacted with various points of the pump wave packet and had experienced some degree of phase modulation $\Delta\phi$ as a result. ΔV_{HF} was extracted by measuring the phase modulation of the probe wave and the following relation,

$$\Delta V_{HF} = \frac{\lambda_{HF} v}{2\pi d}\Delta\phi, \tag{1}$$

where λ_{HF} and v are the ultrasonic wavelength and velocity of the probe wave, respectively, and d is the interaction distance. The phase modulation of the probe SAW was extracted by finding the phase of the peak amplitude of the fast Fourier transform (FFT) of the signal (78 MHz for fused silica and 67 MHz for aluminum). The data were digitally filtered using a Gaussian filter of 0.5, 1 or 2 MHz peak frequency depending on which pump wave was being used and bandwidth of 0.2, 0.4, and 0.66 MHz, respectively.

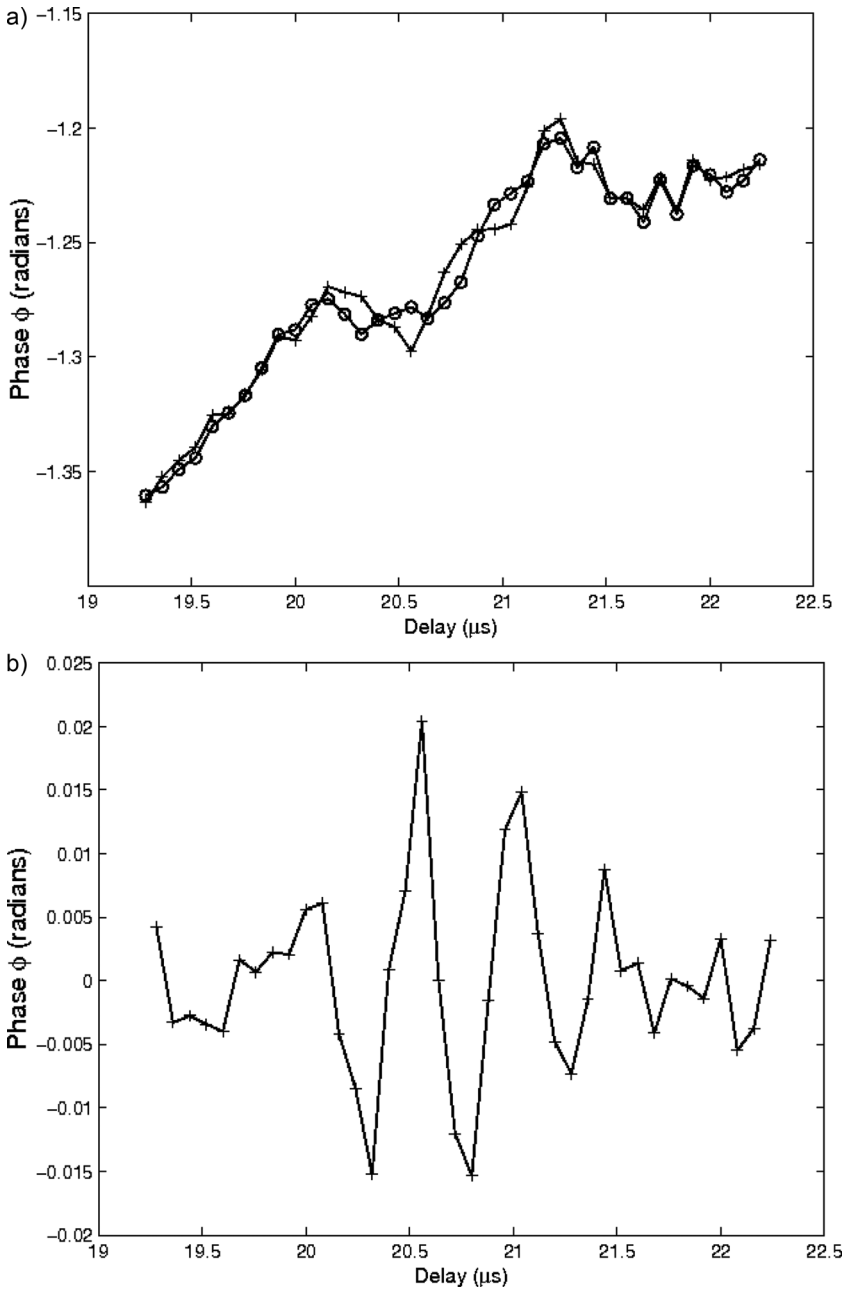

FIG. 3. (a) Phase modulation at "reference" (○) and "target" (+) interaction points with corresponding delay values. (b) Differential probe phase modulation with corresponding delay values, raw data without any digital filtering. The pump SAW frequency was 2 MHz, the probe SAW frequency was 78 MHz and the sample was fused silica.

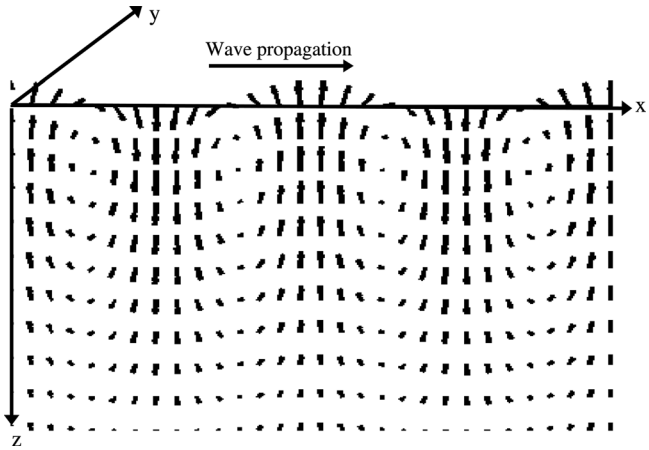

FIG. 4. Particle motion caused by a propagating SAW in the positive x direction.

For the nonlinear experiment presented here, it was important to calculate the stress that was exerted by the pump SAW and was experienced by the probe SAW. The stress is related to the particle displacements[37] and the displacement caused by the pump SAW was measured by means of the Polytec vibrometer. For SAWs there are three components of stress σ_{xx}, σ_{xz}, σ_{zz}, where the x and z axes are defined in Fig. 4.

At the surface of the sample, the σ_{zz} and σ_{xz} components disappear leaving σ_{xx} until a depth of $\sim 0.3\lambda$, where they reach their maximum values.[37] For example, if a 1 MHz pump SAW propagates in a material that has a velocity of 3000 m/s, then the acoustic wavelength (λ_{LF}) of the SAW is 3 mm. A propagating 80 MHz probe SAW in the same material has a wavelength (λ_{HF}) of 37 μm. Since $\lambda_{HF} \ll \lambda_{LF}$, it can be assumed that the probe SAW experiences only the σ_{xx} component. In fact, for the ratio of ultrasonic wavelengths used in this study, σ_{xz} and σ_{zz} are less than 5% of σ_{xx}. σ_{xx} is given by,

$$\sigma_{xx} = \Lambda\left(\frac{\vartheta^2\Phi}{\vartheta x^2} + \frac{\vartheta^2\Phi}{\vartheta z^2}\right) + 2M\left(\frac{\vartheta^2\Phi}{\vartheta x^2} + \frac{\vartheta^2\Psi}{\vartheta x \vartheta z}\right), \tag{2}$$

where Λ and M are the elastic Lamé constants and Φ and Ψ are the scalar and vector potentials of the displacements. Equation 2 was used to convert SAW displacements into stress exerted by the low frequency pump wave on the sample (details are given in the Appendix).

Finally, we calculated the average displacement of the pump wave for the duration of the probe time envelope and converted this into stress since the probe SAW packet had a duration of approximately 0.25 μs; as such, it experienced the average of stresses imposed by the pump wave covered under its time envelope.

Results herein are presented in terms of velocity/stress graphs and the gradient of the velocity/stress data provides a measure of the material nonlinearity. The gradient was calculated using the method of least-squares.

IV. EXPERIMENTAL RESULTS

We conducted two sets of experiments observing pump–probe interaction. They are:

(1) change of pump SAW frequency;
(2) comparison of the nonlinearity response of different materials: aluminum AL-6061 and fused silica.

Results are presented for each of these cases.

A. Changing pump SAW frequency

Three transducers of different frequency were used to generate the pump SAW on a fused silica sample. Transducers with center frequencies of 0.5, 1, and 2.25 MHz were

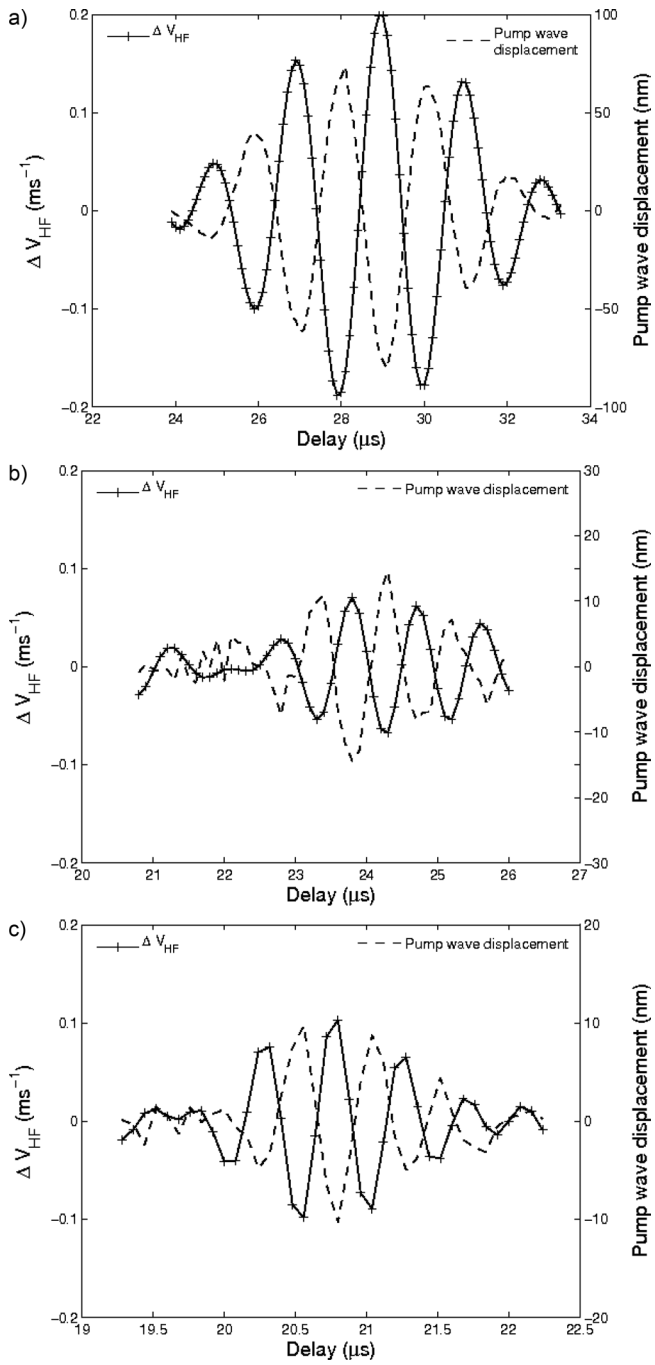

FIG. 5. Experimental velocity modulated probe measurements (+) when interacting with the (a) 0.5 MHz, (b) 1 MHz, and (c) 2 MHz pump SAW (dashed line scaled on right vertical axis) on fused silica. Digitally filtered data using Gaussian filter at 0.5 MHz (filter bandwidth BW = 0.2 MHz), 1 MHz (BW = 0.4 MHz), and 2 MHz (BW = 0.66 MHz), respectively.

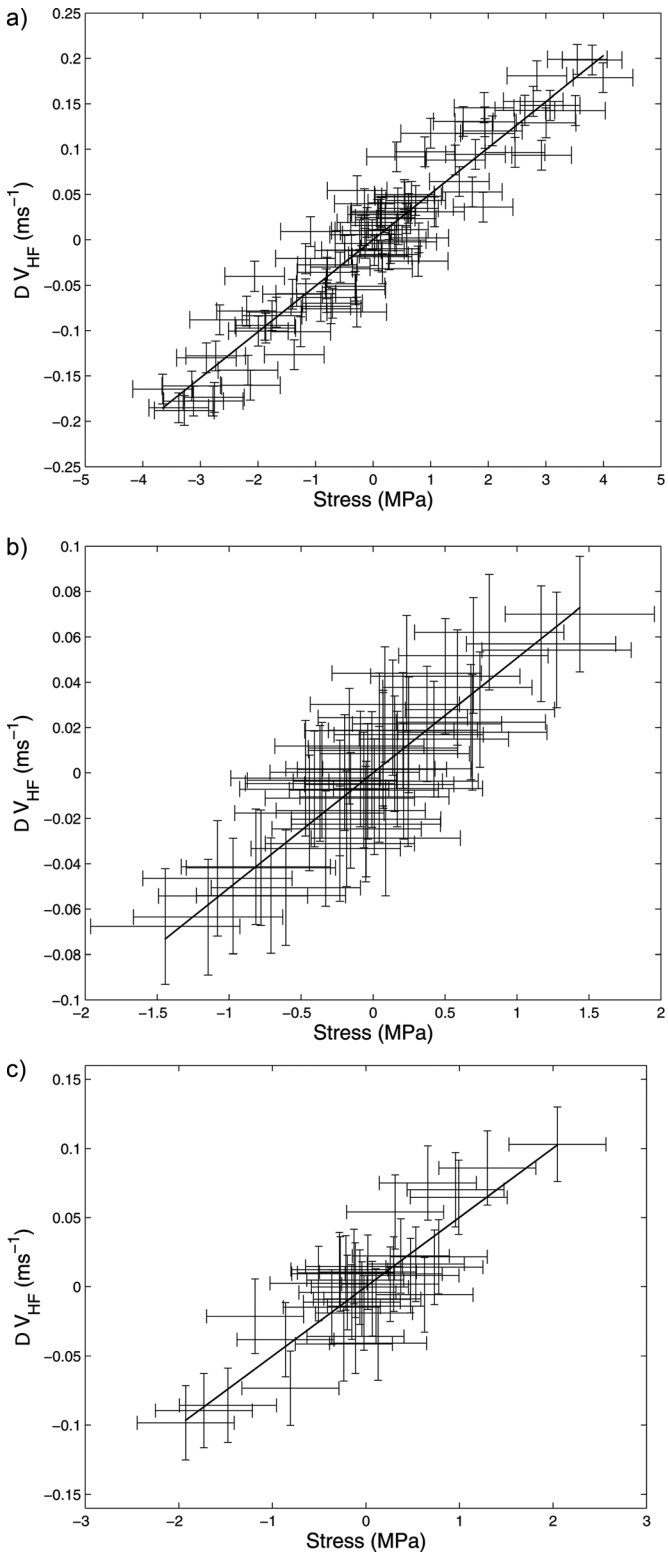

FIG. 6. Velocity plotted against stress for pump frequencies of (a) 0.5 MHz, (b) 1 MHz, and (c) 2 MHz for fused silica. The velocity and stress errors have been plotted. Using the least-squares, a line has been fitted to the data. The gradients of these lines are presented in Table I.

used for this investigation and were excited by a three-cycle sinusoidal burst at frequencies of 0.5, 1, and 2 MHz, respectively. In each case, the probe SAW was delayed in time so that it interacted with multiple points of the pump SAW packet. The delay increments were 80 ns and the interaction distance was 3 mm for all experiments. The phase of the probe SAW at each interaction point was then extracted and converted into velocity change (ΔV_{HF}). Figure 5 shows ΔV_{HF} plotted against the delay in time between the pump and the probe waves for the three different pump frequencies. In the same figure, the dashed line depicts the pump SAW packet displacement. At each frequency, there is a clear correlation between the velocity change and the corresponding pump SAW packet.

TABLE I. Summary of results from all the experiments described in the article.

Material	Pump SAW frequency (MHz)	Probe SAW frequency (MHz)	Gradient (mms^{-1}/MPa)
Fused silica	0.5	78	51 ± 3
Fused silica	1	78	51 ± 7
Fused silica	2	78	50 ± 8
Aluminum AL-6061	1	67	–20 ± 5

In order to compare the three sets of data, the results were plotted in terms of velocity and stress. Figure 6 shows the results including the errors due to the noise of (a) the phase measurements of the probe wave (velocity error) and (b) the displacement of the pump wave measured with the Polytec vibrometer (stress error). The gradients of the lines in Fig. 6 are listed in Table I.

B. Comparison of nonlinear responses between materials: Fused silica and aluminum

Previously reported findings have demonstrated that aluminum and fused silica have opposite nonlinear responses.[6,26,29,38] To validate this, nonlinear experiments were conducted on aluminum AL-6061 and compared with the results from fused silica.

In the experiment the first and last target delays were chosen so that they encapsulated the whole of the 1 MHz pump wave excited by the transducer and 100 ns delay increments were used. The reference delay was set at a time when the pump and probe waves had not interacted.

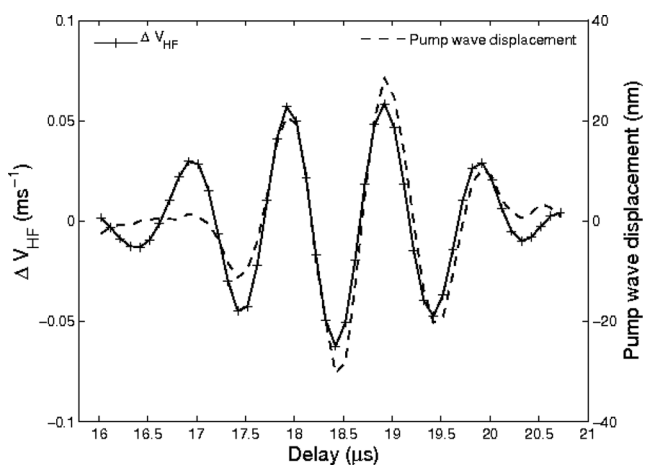

FIG. 7. Experimental velocity modulated probe measurements when interacting with a 1 MHz pump SAW (dashed line scaled on right vertical axis) on aluminum AL-6061. The data have been digitally filtered with a Gaussian filter at 1 MHz (bandwidth 0.4 MHz).

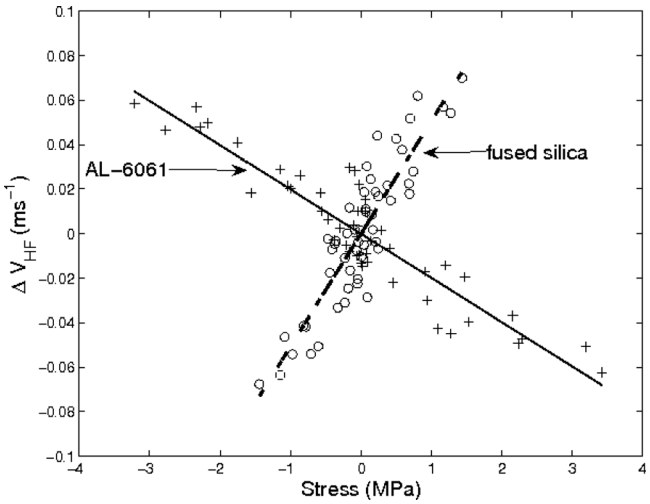

FIG. 8. Velocity plotted against stress for aluminum AL-6061 (+) and fused silica (○). A line has been fitted to the data in each case whose gradient is presented in Table I.

Velocity change measurements for the aluminum are shown in Fig. 7. The results are plotted against stress and compared with results from fused silica in Fig. 8. The gradients of the lines in Fig. 8 are presented in Table I and as expected they have opposite signs for the two materials.

V. CONCLUSIONS

We have demonstrated the capabilities of a nonlinear technique based on parametric interaction of two SAWs to measure material nonlinearity in solids. The technique is based on the frequency mixing of two waves: A low frequency pump wave generated by transducers and a high frequency probe wave generated by a laser. The stress exerted by the pump wave caused a material velocity change, resulting in a phase modulation of the probe signal which was then converted into velocity modulation. Measuring this velocity modulation proved to be challenging as the stresses exerted by the transducer are small (<5 MPa) and required special instrumentation to be developed. Changes in laboratory temperature were found to cause velocity modulations greater than those due to the material intrinsic nonlinearity and an interlacing data acquisition method was developed to suppress this effect. The intrinsic nonlinearity of fused silica was measured using three different pump SAW frequencies. In all cases the ratio of velocity change vs stress was found to be $\sim 50\ \mathrm{mms}^{-1}/\mathrm{MPa}$. Finally, our nonlinear experiments on fused silica and aluminum AL-6061 showed that the relationship between applied stress and velocity change was opposite. The finding agrees with results published from other authors where fused silica was reported to have a negative β-parameter, while metals such as titanium and duraluminum had positive values.[29]

Our experiments were conducted on unfatigued materials. However, as the elastic properties of the material are affected by fatigue, the technique could be applied to measure the residual life of components where the change in gradient is related to the fatigue state of the material. This could form the basis of a technique to extend the usable life of components with major implications for safety and cost savings.

ACKNOWLEDGMENTS

This work has been funded by the UK Research Centre in Non-destructive Evaluation and the UK Technology Strategy Board. The authors would also like to acknowledge Rolls-Royce plc for their support.

APPENDIX: CALCULATION OF σ_{xx} STRESS COMPONENT

In an isotropic medium, a SAW has both longitudinal and shear contributions. Based on the analysis presented in Viktorov,[37] we have found that the σ_{xx} component of stress is related to the displacement with the following relation:

$$\sigma_{xx} = \alpha\left[\Lambda\left(k^2 - q^2\right) + 2Mk^2\left(1 - \frac{2qs}{k^2 + s^2}\right)\right], \tag{A1}$$

where Λ and M are the elastic Lamé constants, k is the pump SAW wavenumber and α is related to the amplitude of the ultrasonic displacement with the following equation:

$$\alpha = \frac{A(k^2 + s^2)}{q(s^2 - k^2)}, \tag{A2}$$

where A is the amplitude of the ultrasonic displacement due to the probe wave, q and s are given by,

$$q = \sqrt{k^2 - k_l^2}, \tag{A3}$$

$$s = \sqrt{k^2 - k_t^2}, \tag{A4}$$

k_l and k_t are the wavenumbers of the longitudinal and transverse mode of the pump SAW, respectively,

$$k_l = \omega\sqrt{\frac{\rho}{\Lambda + 2M}}, \tag{A5}$$

$$k_t = \omega\sqrt{\frac{\rho}{M}}, \tag{A6}$$

with ρ being the material density and ω the pump SAW's angular velocity.

[1]J. Frouin, S. Sathish, T. E. Matikas, and J. K. Na, "Ultrasonic linear and nonlinear behaviour of fatigued Ti-6Al-4V," J. Mater. **14**, 1295–1298 (1999).
[2]P. B. Nagy, G. Blaho, and L. Adler, "Excess nonlinearity in materials containing microcracks," Rev. Prog. Quant. Nondestr. Eval. **13**, 1987–1994 (1994).
[3]K. Jhang and K. Kim, "Evaluation of material degradation using nonlinear acoustic effect," Ultrasonics **37**, 39–44 (1999).
[4]V. V. S. J. Rao, E. Kannan, R. V. Prakash, and K. Balasubramaniam, "Fatigue damage characterization using surface acoustic wave nonlinearity in aluminum alloy AA7175-T7351," J. Appl. Phys. **104**, 123508 (2008).
[5]Y. P. Zheng, R. G. Maev, and I. Y. Solodov, "Nonlinear acoustic applications for material characterisation: A review," Can. J. Phys. **77**, 927–967 (1999).

[6]G. E. Dace, R. B. Thompson, and O. Buck, "Measurement of the acoustic harmonic generation for materials characterization using contact transducers," Rev. Prog. Quant. Nondestr. Eval. **11**, 1685–1692 (1991).
[7]S. Hirsekorn, U. Rabe, and W. Arnold, "Characterization and evaluation of composite laminates by nonlinear ultrasonic transmission measurements," in *Proceedings of ECNDT 2006*, Paper no. Fr.1.5.3, http://www.ndt.net/article/ecndt2006/doc/Fr.1.5.3.pdf (Last viewed May 21, 2010) (2006).
[8]M. Meo, U. Polimeno, and G. Zumpano, "Detecting damage in composite material using nonlinear elastic wave spectroscopy methods," Appl. Compos. Mater. **12**, 115–126 (2008).
[9]K. Van Den Abeele, T. Kathowski, and C. Mattei, "Nonlinear acoustic and ultrasonic NDT of aeronautical components," in *Proceedings of the Innovations in Nonlinear Acoustics: 17th International Symposium on Nonlinear Acoustics*, State Coll., PA, (July 18–22, 2005), pp. 75–78.
[10]K. Van Den Abeele, P. A. Johnson, and A. M. Sutin, "Nonlinear elastic wave spectroscopy (NEWS) techniques to discern material damage, Part I: Nonlinear wave modulation spectroscopy (NWMS)," Res. Nondestruct. Eval. **12**, 17–30 (2000).
[11]P. B. Nagy, "Fatigue damage assessment by nonlinear ultrasonic materials characterization," Ultrasonics **36**, 375–381 (1998).
[12]T. J. Ulrich, A. M. Sutin, and P. A. Johnson, "Imaging and characterising damage using time reversed acoustics," Rev. Prog. Quant. Nondestr. Eval. **26**, 650–656 (2007).
[13]T. J. Ulrich, P. A. Johnson, and A. M. Sutin, "Imaging nonlinear scatterers applying the time reversal mirror," J. Acoust. Soc. Am. **119**, 1514–1518 (2006).
[14]T. Goursolle, S. Dos Santos, O. Bou Matar, and S. Calle, "A two-dimensional pseudospectral model for time reversal and nonlinear elastic wave spectroscopy," J. Acoust. Soc. Am. **122**, 3220–3229 (2007).
[15]V. Yu. Zaitsev, A. M. Sutin, I. Yu. Belyaeva, and V. E. Nazarov, "Nonlinear interaction of acoustical waves due to cracks and its possible usage for cracks detection," J. Vib. Control **1**, 335–344 (1995).
[16]D. A. Cook and Y. H. Berthelot, "Detection of small surface-breaking fatigue cracks in steel using scattering of Rayleigh waves," NDT & E Int. **34**, 483–492 (2001).
[17]Q. Shan and R. J. Dewhurst, "Surface-breaking fatigue crack detection using laser ultrasound," Appl. Phys. Lett. **62**, 2649–2651 (1993).
[18]M. G. Somekh, M. Liu, H. P. Ho, and C. W. See, "An accurate non-contacting laser based system for surface wave velocity measurement," Meas. Sci. Technol. **6**, 1329–1337 (1995).
[19]G. R. Gerhart, "Rayleigh wave velocity for a stress-induced slightly anisotropic solid," J. Acoust. Soc. Am. **60**, 1085–1088 (1976).
[20]M. Duqennoy, M. Ouaftouh, and M. Ourak, "Determination of stresses in aluminium alloy using optical detection of Rayleigh waves," Ultrasonics **37**, 365–372 (1999).
[21]Y. Iwashimizu and O. Kobori, "The Rayleigh wave in a finitely deformed isotropic elastic material," J. Acoust. Soc. Am. **64**, 910–916 (1978).
[22]J. Herrmann, J. Y. Kim, L. J. Jacobs, J. Qu, J. W. Littles, and M. F. Savage, "Assessment of material damage in a nickel-base super alloy using nonlinear Rayleigh surface waves," J. Appl. Phys. **99**, 124913 (2006).
[23]J. L. Blackshire, S. Sathish, J. Na, and J. Frouin, "Nonlinear laser ultrasonic measurements of localized fatigue damage," Rev. Prog. Quant. Nondestr. Eval. **22**, 1479–1487 (2003).
[24]G. Shui, J. Y. Kim, J. Qu, Y. S. Wang, and L. J. Jacobs, "A new technique for measuring the acoustic nonlinearity of materials using Rayleigh waves," NDT & E Int. **41**, 326–329 (2008).
[25]D. M. Donskoy, A. M. Sutin, and A. E. Ekimov, "Nonlinear acoustic interaction on contact interfaces and its use for nondestructive testing," NDT & E Int. **34**, 231–238 (2001).
[26]P. Li, W. P. Winfree, W. T. Yost, and J. H. Cantrell, "Observation of collinear beam-mixing by an amplitude modulated ultrasonic wave in a solid," Proc.-IEEE Ultrason. Symp. 1152–1156 (1983).
[27]A. Moussatov, B. Castagnede, and V. Gusev, "Frequency up-conversion and frequency down-conversion of acoustic waves in damaged materials," Phys. Lett. A **301**, 281–290 (2002).
[28]M. Vila, F. Vender Meulen, S. Dos Santos, L. Haumesser, and O. Bou Matar, "Contact phase modulation method for acoustic nonlinear parameter measurement in solid," Ultrasonics **42**, 1061–1065 (2004).
[29]X. Jacob, C. Barriere, and D. Royer, "Acoustic nonlinearity parameter measurements in solids using the collinear mixing of elastic waves," Appl. Phys. Lett. **82**, 886–888 (2003).
[30]G. Shkerdin and C. Glorieux, "Nonlinear modulation of Lamb modes by clapping delamination," J. Acoust. Soc. Am. **124**, 3397–3409 (2008).
[31]D. M. Donskoy and A. M. Sutin, "Vibro-acoustic modulation nondestructive evaluation technique," J. Intell. Mater. Syst. Struct. **9**, 765–771 (1998).
[32]A. M. Sutin and D. M. Donskoy, "Vibro-acoustic modulation nondestructive evaluation technique," in Proceedings of SPIE Conference on Nondestructive Evaluation of Ageing Aircraft, San Antonio, TX (March 31, 1998), pp. 226–237.
[33]K. Van Den Abeele, A. M. Sutin, J. Carmeliet, and P. A. Johnson, "Microdamage diagnostics using nonlinear elastic wave spectroscopy (NEWS)," NDT & E Int. **34**, 239–248 (2001).
[34]I. J. Collison, T. Stratoudaki, M. Clark, and M. G. Somekh, "Measurement of elastic nonlinearity using remote laser ultrasonics and Cheap Optical Transducers and dual frequency surface acoustic waves," Ultrasonics **48**, 471–477 (2008).
[35]L. Noui and R. J. Dewhurst, "A laser beam deflection technique for the quantitative detection of ultrasonic Lamb waves," Ultrasonics **31**, 425–432 (1993).
[36]K. Salama and C. K. Ling, "The effect of stress on the temperature dependence of ultrasonic velocity," J. Appl. Phys. **51**, 1505–1509 (1980).
[37]I. A. Viktorov, *Rayleigh and Lamb Waves: Physical Theory and Applications* (Plenum Press, New York, 1967), Chap. 1, pp. 1–7.
[38]R. B. Thompson, O. Buck, and D. O. Thompson, "Higher harmonics of finite amplitude ultrasonic waves in solids," J. Acoust. Soc. Am. **59**, 1087–1094 (1976).